RSC Advances

PAPER

View Article Online
View Journal | View Issue

Cite this: *RSC Adv.*, 2023, **13**, 32842

Two novel low molecular weight gelator-driven supramolecular metallogels efficient in antimicrobial activity applications†

Subhendu Dhibar,‡*[a] Suchetana Pal,‡[b] Kripasindhu Karmakar,[a] Sk Abdul Hafiz,[c] Subham Bhattacharjee,[c] Arpita Roy,[d] S. K. Mehebub Rahaman,[a] Soumya Jyoti Ray,[d] Somasri Dam*[b] and Bidyut Saha*[a]

A remarkable ultrasonication technique was successfully employed to create two novel metallogels using citric acid as a low molecular weight gelator, in combination with cadmium(II)-acetate and mercury(II)-acetate dissolved in *N*,*N*-dimethyl formamide at room temperature and under ambient conditions. The mechanical properties of the resulting Cd(II)- and Hg(II)–metallogels were rigorously examined through rheological analyses, which revealed their robust mechanical stability under varying angular frequencies and shear strains. Detailed characterization of the chemical constituents within these metallogels was accomplished through EDX mapping experiments, while microstructural features were visualized using field emission scanning electron microscope (FESEM) images. Additionally, FT-IR spectroscopic analysis was employed to elucidate the metallogel formation mechanism. Significantly, the antimicrobial efficacy of these novel metallogels was assessed against a panel of bacteria, including Gram-positive strains such as *Bacillus subtilis* and *Staphylococcus epidermidis*, as well as Gram-negative species like *Escherichia coli* and *Pseudomonas aeruginosa*. The results demonstrated substantial antibacterial activity, highlighting the potential of Cd(II) and Hg(II)-based citric acid-mediated metallogels as effective agents against a broad spectrum of bacteria. In conclusion, this study provides a comprehensive exploration of the synthesis, characterization, and antimicrobial properties of Cd(II) and Hg(II)-based citric acid-mediated metallogels, shedding light on their promising applications in combating both Gram-positive and Gram-negative bacterial infections. These findings open up exciting prospects for the development of advanced materials with multifaceted industrial and biomedical uses.

Received 25th July 2023
Accepted 8th October 2023

DOI: 10.1039/d3ra05019j

rsc.li/rsc-advances

1. Introduction

Gels are ubiquitous in daily life, present in diverse forms of consumer product, like hair gels, toothpaste, shampoo and soap, as well as contact lenses and various wound healing ointments.[1] Gels are often thought to consist of an elastic cross-linked network and the trapped liquid. Although mostly liquid, they have a solid-like rheology; generally, gels comprise 99% (w/v) liquid, with the remaining portion being the gelator.[1,2] A gel can be commonly recognized through its stability against gravitational force *via* an inversion vial test.[3] In terms of the forces that cause gelation, gels may be divided into two categories: physical gels or supramolecular gels, in which intermolecular interactions lead to gel formation, and chemical gels, in which covalent bonds cross-link the gel skeleton.[1] In recent years, supramolecular gels have drawn a lot of interest from researchers due to their extensive applications in the scientific arena. Self-assembly of low molecular weight gelators (LMWGs) and solvent molecules *via* different types of non-covalent interactions such as hydrogen bonding,[4] π···π stacking,[1] hydrophobic interactions,[2,5] metal coordination,[6] electrostatic interactions,[7] aromatic π-ring-mediated interactions,[2,5] van der Waals forces,[3] π-system-based stacking,[8] hydrophobic,[9] hydrophilic or dipole–dipole interactions[10] *etc.* plays a dynamic role in supramolecular gelation. The literature is full of reports on supramolecular gelation mediated by numerous solvents, including water,[11] alcohols,[12,13] dimethyl sulfoxide,[14] acetonitrile,[15] dimethylformamide,[16] carbon tetrachloride,[17] 1,2-dichlorobenzene,[18,19] tetrahydrofuran,[20] acetone,[14] deuterated dichloromethane,[21] dichloromethane,[22] toluene,[23] *etc.* Supramolecular metallogels have great application prospects in conduction,[24] redox,[25] catalysis,[26–28] sensing,[29,30] proton

[a]*Colloid Chemistry Laboratory, Department of Chemistry, The University of Burdwan, Golapbag, Burdwan-713104, West Bengal, India. E-mail: sdhibar@scholar.buruniv.ac.in; bsaha@chem.buruniv.ac.in; Tel: +91 7001575909; +91 9476341691*

[b]*Department of Microbiology, The University of Burdwan, Burdwan-713104, West Bengal, India. E-mail: sdam@microbio.buruniv.ac.in*

[c]*Department of Chemistry, Kazi Nazrul University, Asansol-713303, West Bengal, India*

[d]*Department of Physics, Indian Institute of Technology Patna, Bihar-801106, India*

† Electronic supplementary information (ESI) available. See DOI: https://doi.org/10.1039/d3ra05019j

‡ SD and SP should be treated as joint first authors.

conductivity,[31,32] magnetism,[33] and nanoparticle templating,[34] due to the essential participation of metal ions in the gel network.

The metallogel formation process concentrates on a metal coordination complex,[1,2] coordination polymeric networks,[35–37] cross-linked coordination polymers,[38] organometallics[39] and metal–ligand interaction-mediated gelation[40] *etc.* Metal ions are a key constituent in metallogel networks in the form of coordinated metal ions (in a discrete coordination complex), cross-linking metal nodes with coordinating ligands (in coordination polymers), and metal nanoparticles anchored to the gel network. Innumerable LMWGs are well-known; for example, amino acid,[41] nucleic acid,[42] steroid,[43] peptide,[44] carbohydrate,[45] stearic acid,[46] sorbitol,[47] amino acid,[48] fatty acid,[49] dendrimer,[50] bile acid,[51] and carboxylic acid-mediated gelators are really outstanding in gel chemistry.[16] Broadly, the role of dicarboxylic acids in metallogel-research is highly precious.[16] Scientists have established cell imaging,[52] photodynamic therapy,[53] chemotherapy,[54] antibacterial activity and biological benefits by using metallogel systems containing different metal ions. Due to its effectiveness, citric acid is well-established as an important gelator to offer functional supramolecular gel-frameworks. Citric acid, which has a relatively low toxin level, is mostly employed as a flavouring and preservative in food and beverages, giving fruit and soft drinks a sour flavour. In addition to being utilised in medicines and domestic cleaning products, tablets, ointments, and cosmetic preparations, citric acid is also employed to store blood. It serves as both an antioxidant and a bacterial habitant. The deep context of citric acid opens up the possibility of forming functional supramolecular metallogels with a high aspect ratio. The proposed idea regarding citric acid has been experimentally carried out and implemented through current efforts. Moreover, the consequence of Cd(II)-mediated materials in biological investigation is well accepted.[55–57] Recently, researchers have also been trying to explore the antibacterial activity of Cd(II)-based systems.[54] The value of Hg(II)-directed materials in biological systems is also recognized.[58–60] Following these trends, we obtained inspiration to study the impacts of such metallogel scaffolds against pathogens. In this work, we have investigated citric acid's tendency towards metallo-gelation with Cd(II)- and Hg(II)-sources in *N*,*N*-dimethyl formamide solvent under ambient conditions. Citric acid, an LMWG, leads to the formation of two novel supramolecular metallogels, namely Cd(II)–citric acid metallogel (Cd–CA) and Hg(II)–citric acid metallogel (Hg–CA). The mechanical properties of the synthesized Cd–CA and Hg–CA metallogels were characterized through rheological analysis. The morphological patterns of the synthesized metallogels are exposed through FESEM study and chemical constitute elements are characterized through EDX mapping investigations. The excessive usage of conventional antibiotics has culminated in the development of drug-resistant organisms. As a result, the urgency to develop new antimicrobial agents is a major concern. Metallogel moieties may serve as promising candidates to inhibit bacterial growth, making them appealing in the biomedical sector. Citric acid's effect in biological applications motivated us to identify the anticipated bio-functionality of citric acid and various metal ion-based metallogel systems. Thus, the current efforts have shown the anti-bacterial efficacy of citric acid-based metallogels of Cd(II) and Hg(II).

2. Experimental

2.1. Materials

Cadmium(II) acetate dihydrate (99.995%), mercury(II) acetate (≥98.0%) and citric acid were bought from Merck Chemical Company and used without further purification. Dry DMF solvent was used throughout the work. Tryptone, anhydrous D-(+)-glucose and yeast extract powder were purchased from Himedia.

2.2. Apparatus and measurements

A PHUC-150 Phoenix Digital Ultrasonic Cleaner was used in metallogel synthesis. The rheological experiment was carried out using a rheometer (TA Instrument) with a cone plate shape. The field emission scanning electron microscope (FESEM) investigation was carried out using a Carl Zeiss SUPRA 55VP FESEM instrument. ZEISS, EVO 18 apparatus was used to perform the scanning mode energy-dispersive X-ray spectroscopy (EDX) studies. Topography analysis was executed through an atomic force microscope (Agilent Technology 5500) in noncontact mode by a silicon tip. To analyse the FTIR spectrum of the metallogel, a JASCO FTIR 4700 spectrometer was employed.

2.3. Synthesis of Cd(II)–citric acid (Cd–CA) and Hg(II)–citric acid (Hg–CA)-based metallogels

The white colour, stable Cd–CA metallogel was prepared by the rapid mixing of 1 mL of a DMF solution of cadmium acetate (1 mmol, 0.266 g) and 1 mL of a DMF solution of citric acid (1 mmol, 0.192 g), followed by continuous water bath ultrasonication for ten minutes (Fig. 1). Following the same synthetic protocol, a white colour, stable Hg–CA metallogel was prepared by mixing 1 mL of a DMF solution of mercury acetate

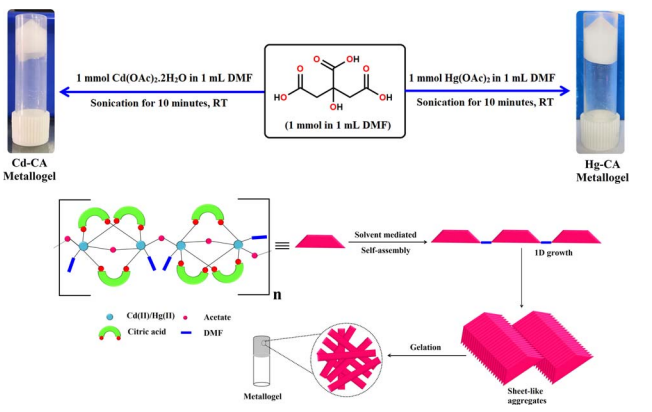

Fig. 1 Schematic representation of the probable synthetic route and gelation mechanism of the Cd(II)–metallogel (Cd–CA) and Hg(II)–metallogel (Hg–CA) and their inverted photography images showing the stability of the gel materials.

(1 mmol, 0.318 g) and 1 mL of a DMF solution of citric acid (1 mmol, 0.192 g), followed by ultra-sonication for ten minutes (Fig. 1). The formation of a supramolecular network occurred through non-covalent interactions between the metal ions (cadmium or mercury) and citric acid in the solvent (DMF), leading to the formation of a stable three-dimensional network. Ultrasonication helps in speeding up the gelation process by improving the mixing and assembly of these components (Fig. 1).

2.4. Calculation of the minimum critical gelation concentration (MGC) of the Cd–CA and Hg–CA metallogels

We have evaluated the minimal critical gelation concentration (MGC) of the Cd–CA and Hg–CA metallogels. To determine the MGC of the Co–AIA metallogel, the concentrations of $Cd(CH_3COO)_2\cdot 2H_2O$ and citric acid were changed within a narrow range (*i.e.* 10–266 mg mL^{-1}). For this assessment, [$Cd(CH_3COO)_2\cdot 2H_2O$] : [citric acid] was kept at a constant molar ratio of 1 : 1, in order to form a Cd–CA metallogel. At a concentration of 266 mg mL^{-1} of Cd(II)-acetate salt and citric acid in DMF solvent, a stable, white-coloured metallogel, Cd–CA, was obtained. To evaluate the MGC of the Hg–CA metallogel, the concentrations of $Hg(CH_3COO)_2$ salt and citric acid were changed from 10–318 mg mL^{-1}. At a concentration of 318 mg mL^{-1} of Cd(II)-acetate salt and citric acid in DMF solvent, a stable Hg–CA metallogel was formed.

2.5. Antimicrobial activity of the metallogels

The metallogels were tested for bacterial susceptibility after being suspended in sterile water at a concentration of 100 mg mL^{-1}. The antibacterial potency of each metallogel was evaluated against Gram-positive *Bacillus subtilis* (*B. subtilis*) and *Staphylococcus epidermidis* (*S. epidermidis*), and Gram-negative *Escherichia coli* (*E. coli*) and *Pseudomonas aeruginosa* (*P. aeruginosa*). Streptomycin was used as positive control as it inhibits both Gram-positive and Gram-negative bacteria. Citric acid has intrinsic antimicrobial properties. However, it requires a minimum inhibitory concentration to have an antagonistic effect on microorganisms. In the literature, the inhibitory concentrations of citric acid are reported to be 900 mg mL^{-1} for *Staphylococcus aureus* and 1500 mg mL^{-1} for *Escherichia coli* (PMID 18436609). In another report, it was found to be 0.06 g mL^{-1} for *Escherichia coli* and 0.03 g mL^{-1} for *Staphylococcus aureus*.[61] In our study, 1 mM citric acid in 1 mL of DMF was used to prepare metallogels. To check the antimicrobial effect of citric acid, 1 mM citric acid was tested as a negative control. A 100 μL sample of a log phase culture of each bacterial inoculum was spread uniformly on TGE (1% tryptone, 1% glucose, and 1% yeast extract; pH 6.5) agar plates using sterile cotton swabs. Then, 10 μL of each metallogel suspension was spotted across the surface of the agar plates. Further, 10 μL of 1 mM citric acid was also spotted across the surface of the agar plates that were spread with bacterial inoculum. The plates were kept at 37 °C for 24 hours.[62] Each experiment was carried out in triplicate.

3. Results and discussion

3.1. Rheological analysis

To evaluate the mechanical stability of the Cd–CA metallogel and Hg–CA metallogel, angular frequency and strain-sweep-dependent rheological analysis was performed. When the reading of the storage modulus (G') of the gel sample is confirmed to be larger than the loss modulus (G''), then the visco-elastic nature of the material is confirmed. The Cd–CA and Hg–CA metallogel have a gel nature and exhibit semi-solid-like behaviour since $G' > G''$. Cd–CA metallogel has a high tolerance limit, which is supported by the fact that its average storage modulus ($G' > 10^5$ Pa) is much greater than its loss modulus (G'') (Fig. 2). The findings of a strain-sweep measurement of the Cd–CA metallogel material obtained at a fixed frequency of 6.283 rad s^{-1} are shown in Fig. 3.

Experimental rheology on a Hg–CA metallogel at a fixed concentration of $Hg(CH_3COO)_2$ salt and citric acid (*i.e.* MGC = 318 mg mL^{-1}) revealed that the storage modulus (G') was much higher than the loss modulus (G'') (*i.e.* $G' > G''$) (Fig. 4). As shown by the rheological data, the Hg–CA metallogel retains its gel structural structure and exhibits solid-like behaviour since its average storage modulus (G') is so much greater than its loss modulus (G'') (Fig. 4). Fig. 5 depicts a strain-sweep experiment performed on Hg–CA metallogel material at a constant frequency of 6.27997 rad s^{-1}. The results from the strain-sweep experiment show that the critical strain, the lowest strain for gel breakdown of the Hg–CA metallogel, occurs at a strain of 0.45%, when G' mixes with G'' (Fig. 5).

3.2. Morphological study

The morphological characteristics of the Cd–CA and Hg–CA metallogels were elucidated using FESEM images. In the FESEM image of the Cd–CA metallogel (Fig. 6a), a distinct network composed of agglomerated nano-rods was prominently evident. This structural arrangement in the metallogel was a result of the interaction between $Cd(CH_3COO)_2\cdot 2H_2O$ and citric acid in DMF medium, as observed in the FESEM patterns. The prevalence of supramolecular interactions between $Cd(CH_3COO)_2\cdot 2H_2O$ and

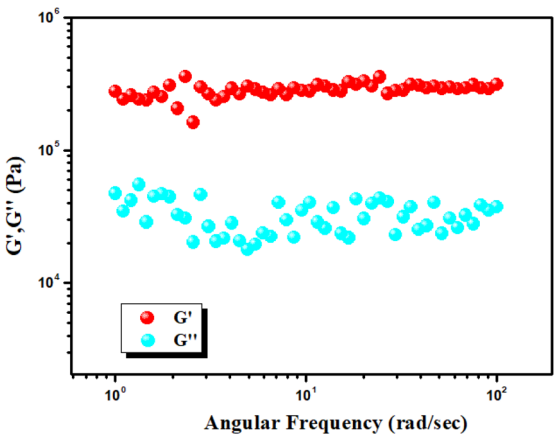

Fig. 2 Plot of G' and G'' of the Cd(II) metallogel *vs.* angular frequency.

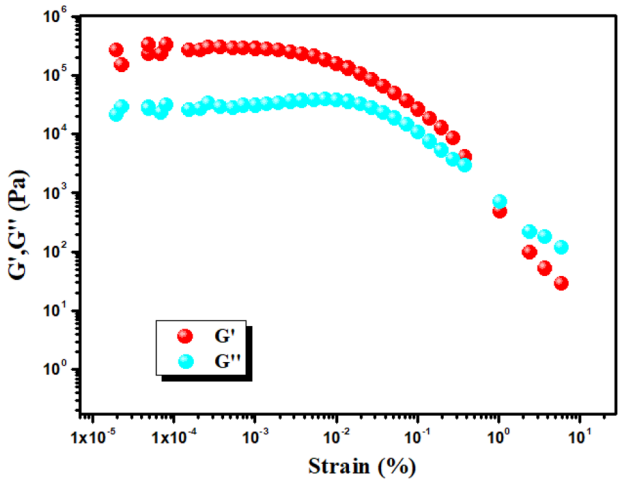

Fig. 3 Strain-sweep measurements of the Cd–CA metallogel.

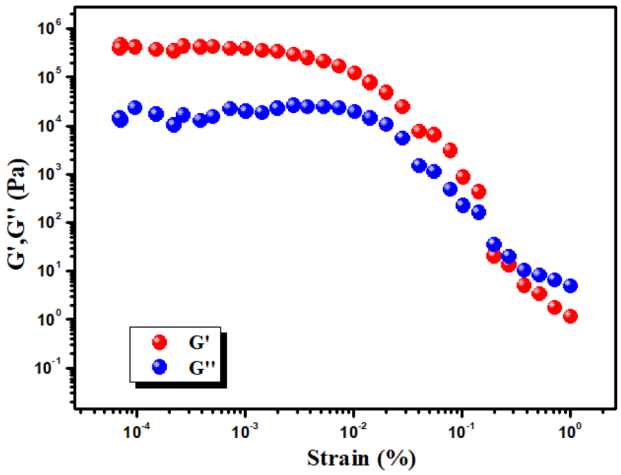

Fig. 5 Strain-sweep measurements of the Hg–CA metallogel.

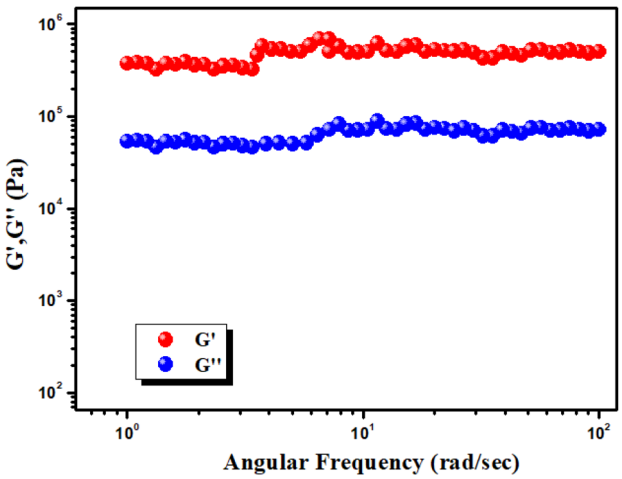

Fig. 4 Plot of G' and G'' of the Hg(II) metallogel *Vs* angular frequency.

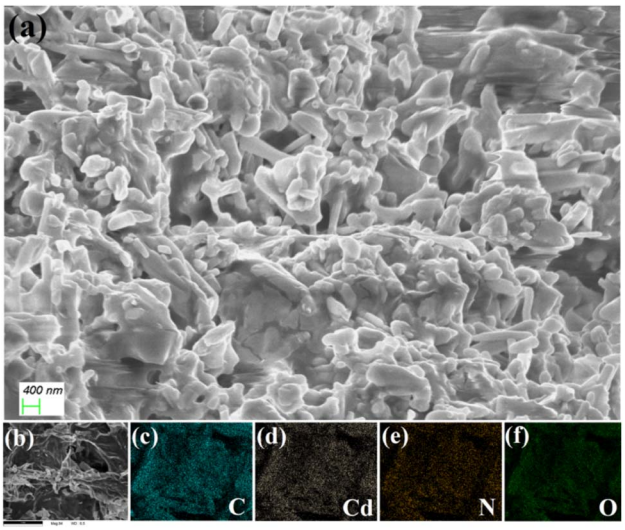

Fig. 6 (a) The Cd–CA metallogel's FESEM microstructural characteristics, and (b–f) the C, Cd, N, and O elements present in the elemental mapping of the Cd–CA metallogel.

citric acid in DMF medium contributed to the formation of these microstructural networks (please see Fig. S1 in the ESI† for supplementary field emission scanning electron microscopy (FESEM) images of the Cd–CA metallogel). The chemical constituents of the Cd–CA metallogel are confirmed through EDX elemental mapping experiments. In Fig. 6b–f, EDX analysis confirms that the main chemical constituents of the Cd–CA metallogel were C, Cd, N, and O elements. In contrast, an agglomerated nano-flake like architecture was exposed through FESEM analysis of the Hg–CA metallogel (Fig. 7a) (please see Fig. S1 in the ESI† for supplementary field emission scanning electron microscopy (FESEM) images of the Hg–CA metallogel). The main gel forming elements were confirmed through EDX elemental mapping. Fig. 7b–f show the presence of the main gel forming elements, *i.e.* C, Hg, N and O, of the Hg–CA metallogel. Please see supplementary figures, *i.e.* Fig. S3 and S4 in the ESI,† for atomic force microscopy (AFM) images depicting the Cd–CA and Hg–CA metallogels. These AFM images reveal the presence of minute metallogel particles that are dispersed across the surface.

3.3. FT-IR analysis of the Cd–CA and Hg–CA metallogels

FTIR spectroscopy is used for analysing the emission and absorption of the Cd–CA and Hg–CA gel materials in the infrared (IR) region (Fig. 8). Functional groups present in the material have fingerprint vibrations. Assignment of these vibration bands is used for confirming the presence of these groups. These vibrations shift to shorter wavelengths or longer wavelengths depending on the change in the microenvironment of the material. The significant spectral absorption bands of the Cd–CA metallogel are seen, with O–H stretching in hydroxyl groups accounting for the wide and broad peak at 3450 cm^{-1}

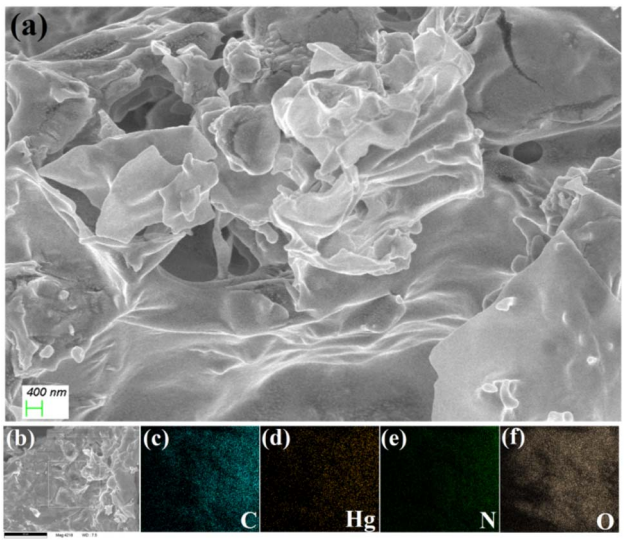

Fig. 7 (a) The Hg–CA metallogel's FESEM microstructural characteristics, and (b–f) the C, Hg, N, and O elements present in the elemental mapping of the Hg–CA metallogel.

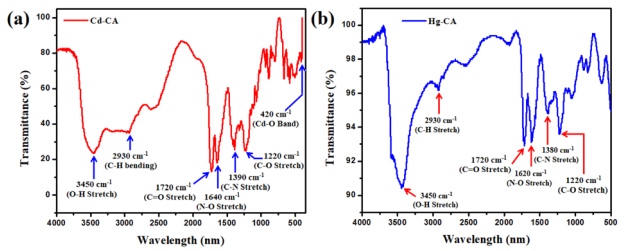

Fig. 8 (a and b) FT-IR Spectra of Cd–CA and Hg–CA metallogel in their xerogel form.

(Fig. 8a). The vibrational mode at 2930 cm^{-1} is attributed to symmetric C–H bonds. According to the scientific literature, the carboxyl C=O stretching in carboxyl groups is associated with the peaks at 1720 cm^{-1}. The vibrational modes associated with the peaks at 1640 cm^{-1}, 1390 cm^{-1}, and 1220 cm^{-1} are N–O stretching, C–N stretching, and C–O stretching, respectively (Fig. 8a). To further prove the strength of the connection between citric acid and the DMF-soluble cadmium acetate, a peak at 420 cm^{-1} can be observed in the spectrum (Fig. 8a), which is created owing to the presence of the Cd–O bond in the formed metallogel. The significant spectral absorption bands of the Hg–CA metallogel are also seen, with O–H stretching in hydroxyl groups accounting for the wide and broad peak at 3450 cm^{-1} (Fig. 8b). The vibrational mode at 2930 cm^{-1} is attributed to symmetric C–H bonds. According to the scientific literature, the carboxyl C=O stretching in carboxyl groups is associated with the peaks at 1720 cm^{-1}. The vibrational modes associated with the peaks at 1620 cm^{-1}, 1380 cm^{-1}, and 1220 cm^{-1} are N–O stretching, C–N stretching, and C–O stretching, respectively (Fig. 8b).

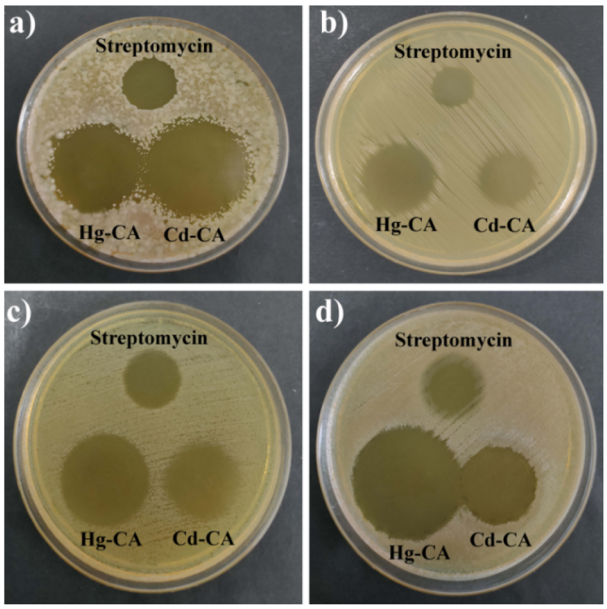

Fig. 9 Antimicrobial activity of Hg–CA and Cd–CA against four pathogenic strains: (a) *B. subtilis*, (b) *S. epidermidis*, (c) *E. coli* and (d) *P. aeruginosa*.

Table 1 Antimicrobial activity of the metallogels[a]

Bacterial strain (s)	Zone of inhibition against streptomycin (mm in diameter)
B. subtilis	19.16 ± 0.28
S. epidermidis	14.33 ± 0.57
E. coli	19.5 ± 0.5
P. aeruginosa	19.33 ± 0.28

Bacterial strain (s)	Volume of metallogel (μL)	Concentration of metallogel (mg mL^{-1})	Zone of inhibition (mm in diameter)	
			Hg–CA	Cd–CA
B. subtilis	10	100	30.16 ± 0.28	35.13 ± 0.23
S. epidermidis	10	100	23.5 ± 0.5	16.83 ± 0.28
E. coli	10	100	29.33 ± 0.57	24.66 ± 0.57
P. aeruginosa	10	100	35.83 ± 0.28	24.33 ± 0.28

[a] ± standard deviation.

3.4. Inhibiting activity for pathogens

Hg–CA and Cd–CA both showed strong antibacterial activity against Gram-positive *B. subtilis*, *S. epidermidis* and Gram-negative *E. coli*, *P. aeruginosa* (Fig. 9, Table 1). The formation of inhibitory zones following contact with metal based gels suggests that they have the potential to be utilized as broad-spectrum antibacterial agents. However, there was no inhibition zone found in the plates spotted with 1 mM citric acid, demonstrating that the inhibition zones reported with Hg–CA and Cd–CA were not caused by citric acid's antibacterial properties (Fig. 10).

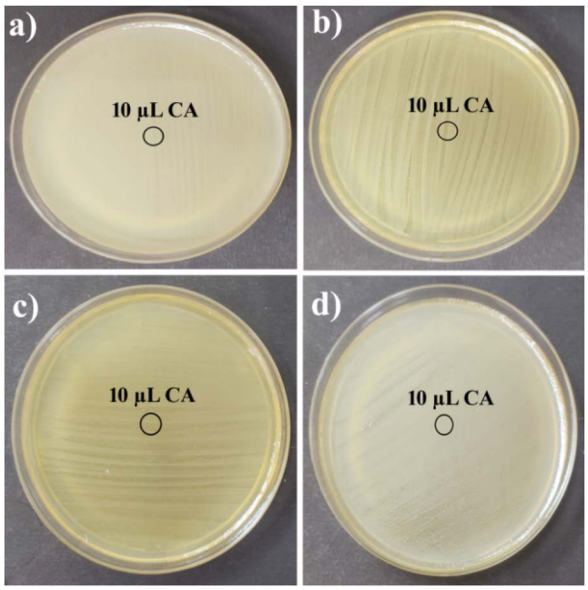

Fig. 10 No inhibition zone was observed for the plates spread with (a) *B. subtilis*, (b) *S. epidermidis*, (c) *E. coli* and (d) *P. aeruginosa* spotted with 1 mM citric acid.

4. Conclusions

In summary, this study successfully synthesized two innovative metallogels through a straightforward process involving the direct mixing of cadmium acetate dihydrate and mercury acetate solutions with citric acid, followed by ultrasonication at room temperature. Our investigation revealed distinct morphological patterns in the Cd(II) and Hg(II)-based metallogel samples through FESEM microstructural analysis. Furthermore, the mechanical stability of these materials was confirmed *via* rheological tests. FT-IR spectroscopy shed light on potential intermolecular interactions within the gel structures. Most notably, our experimental findings underscore the significant potential of both Cd(II) and Hg(II)–metallogels as formidable candidates for inhibiting the growth of harmful and even lethal bacteria. The antibacterial assays conducted in this study have demonstrated the promising applicability of these metallogels across a spectrum of industries, with particularly advanced applications foreseen in the biomedical and pharmaceutical sectors. In conclusion, these novel metallogels not only broaden the horizon of material synthesis but also hold immense promise in addressing critical challenges related to bacterial infections, offering a new avenue for innovative solutions in diverse fields where antimicrobial properties are paramount. As such, they represent a valuable asset in the ongoing pursuit of advancements in science and technology. These materials stand as formidable contenders in the battle against harmful and even life-threatening bacteria. With applications extending across diverse industries, including promising prospects in biomedicine and pharmaceuticals, these metallogels represent a pivotal step toward innovative solutions for some of the most pressing challenges in our society. Looking ahead, the synthesis protocol developed in this study holds immense promise for further exploration and application. Future research can delve into the fine-tuning of these metallogels for specific uses, while interdisciplinary collaborations can propel their integration into practical solutions for healthcare, environmental protection, and advanced materials science. As such, the impact of this work extends far beyond the laboratory, offering a transformative pathway for advancements in science and technology with far-reaching benefits for society.

Conflicts of interest

The authors declare no competing financial interests.

Acknowledgements

S. D. is grateful to the UGC, New Delhi, for awarding him a Dr DS Kothari Postdoctoral Fellowship (award letter number: F.4-2/2006 (BSR)/CH/19-20/0224). S. P. acknowledges University Grants Commission (UGC), Government of India for the Senior Research Fellowship (award letter number: 16-6(DEC.2018)/2019(NET/CSIR)). S. B. thankfully acknowledges the DST Inspire Faculty Research Grant (Faculty Registration No. IFA18-CH304; DST/INSPIRE/04/2018/000329).

Notes and references

1 N. M. Sangeetha and U. Maitra, *Chem. Soc. Rev.*, 2005, **34**, 821–836.
2 P. Dastidar, *Chem. Soc. Rev.*, 2008, **37**, 2699–2715.
3 S. Dhibar, A. Dey, S. Majumdar, D. Ghosh, P. P. Ray and B. Dey, *ACS Appl. Electron. Mater.*, 2019, **1**, 1899–1908.
4 R. G. Weiss and P. Terech, *Molecular Gels: Materials with Self-Assembled Fibrillar Networks*, Springer, Dordrecht, 2005.
5 (*a*) A. Y.-Y. Tam and V. W.-W. Yam, *Chem. Soc. Rev.*, 2013, **42**, 1540–1567; (*b*) C. Tomasini and N. Castellucci, *Chem. Soc. Rev.*, 2013, **42**, 156–172; (*c*) L. Meazza, J. A. Foster, K. Fucke, P. Metrangolo, G. Resnati and J. W. Steed, *Nat. Chem.*, 2013, **5**, 42–47.
6 (*a*) Q. Wang, J. L. Mynar, M. Yoshida, E. Lee, M. Lee, K. Okuro, K. Kinbara and T. Aida, *Nature*, 2010, **436**, 339–343; (*b*) N. Holten-Andersen, M. J. Harrington, H. Birkedal, B. P. Lee, P. B. Messersmith, K. Y. C. Lee and J. H. Waite, *Proc. Natl. Acad. Sci. U. S. A.*, 2011, **108**, 2651–2655; (*c*) M. Burnworth, L. Tang, J. R. Kumpfer, A. J. Duncan, F. L. Beyer, G. L. Fiore, S. J. Rowan and C. Weder, *Nature*, 2011, **472**, 334–337; (*d*) P. Cordier, F. Tournilhac, C. Soulie-Ziakovic and L. Leibler, *Nature*, 2008, **451**, 977–980.
7 (*a*) T.-A. Asoh and A. Kikuchi, *Chem. Commun.*, 2012, **48**, 10019–10021; (*b*) X. Wang, F. Liu, X. Zheng and J. Sun, *Angew. Chem., Int. Ed.*, 2011, **50**, 11378–11381; (*c*) H. Wang, M. B. Hansen, D. W. P. M. Löwik, J. C. M. van Hest, Y. Li, J. A. Jansen and S. C. G. Leeuwenburgh, *Adv. Mater.*, 2011, **23**, H119–H124.
8 (*a*) Y. Xu, Q. Wu, Y. Sun, H. Bai and G. Shi, *ACS Nano*, 2010, **4**, 7358–7362; (*b*) S. Burattini, B. W. Greenland, D. H. Merino, W. Weng, J. Seppala, H. M. Colquhoun, W. Hayes,

M. E. Mackay, I. W. HamLey and S. J. Rowan, *J. Am. Chem. Soc.*, 2010, **132**, 12051–12058.

9 (*a*) A. Harada, R. Kobayashi, Y. Takashima, A. Hashidzume and H. Yamaguchi, *Nat. Chem.*, 2011, **3**, 34–37; (*b*) T. Park and S. C. Zimmerman, *J. Am. Chem. Soc.*, 2006, **128**, 11582–11590.

10 (*a*) M. Shirakawa, N. Fujita and S. Shinkai, *J. Am. Chem. Soc.*, 2003, **125**, 9902–9903; (*b*) J. R. Moffat, G. J. Seeley, J. T. Carter, A. Burgess and D. K. Smith, *Chem. Commun.*, 2008, 4601–4603.

11 (*a*) S. Dhibar, D. Ghosh, S. Majumdar and B. Dey, *ACS Omega*, 2020, **5**, 2680–2689; (*b*) S. Dhibar, A. Dey, R. Jana, A. Chatterjee, G. K. Das, P. P. Ray and B. Dey, *Dalton Trans.*, 2019, **48**, 17388–17394; (*c*) S. Dhibar, R. Jana, P. P. Ray and B. Dey, *J. Mol. Liq.*, 2019, **289**, 111–126; (*d*) S. Dhibar, A. Dey, D. Ghosh, A. Mandal and B. Dey, *J. Mol. Liq.*, 2019, **276**, 184–193; (*e*) S. Dhibar, A. Dey, A. Dey, S. Majumdar, A. Mandal, P. P. Ray and B. Dey, *New J. Chem.*, 2019, **43**, 15691–15699; (*f*) D. Ghosh, S. Dhibar, A. Dey, S. Mukherjee, N. Joardar, S. P. Sinha Babu and B. Dey, *J. Mol. Liq.*, 2019, **280**, 1–12; (*g*) S. Majumdar, T. Singha, S. Dhibar, A. Mandal, P. K. Datta and B. Dey, *ACS Appl. Electron. Mater.*, 2020, **2**, 3678–3685; (*h*) S. Majumdar, A. Dey, R. Sahu, S. Dhibar, P. P. Ray and B. Dey, *ACS Appl. Nano Mater.*, 2020, **3**, 11025–11036; (*i*) S. Dhibar, A. Dey, S. Majumdar, D. Ghosh, P. P. Ray and B. Dey, *ACS Appl. Electron. Mater.*, 2019, **1**, 1899–1908.

12 (*a*) Q. Lin, Q.-P. Yang, B. Sun, Y.-P. Fu, X. Zhu, T.-B. Wei and Y.-M. Zhang, *Soft Matter*, 2014, **10**, 8427–8432; (*b*) A. M. Amacher, J. Puigmartí-Luis, Y. Geng, V. Lebedev, V. Laukhin, K. Kramer, J. Hauser, D. B. Amabilino, S. Decurtins and S.-X. Decurtins, *Chem. Commun.*, 2015, **51**, 16421; (*c*) S. Sarkar, S. Dutta, P. Bairi and T. Pal, *Langmuir*, 2014, **30**, 7833–7841.

13 (*a*) C. K. Karan and M. Bhattacharjee, *ACS Appl. Mater. Interfaces*, 2016, **8**, 5526–5535; (*b*) S. Dey, D. Datta, K. Chakraborty, S. Nandi, A. Anoop and T. Pathak, *RSC Adv.*, 2013, **3**, 9163–9166; (*c*) M.-O. M. Piepenbrock, N. Clarke and J. W. Steed, *Soft Matter*, 2010, **6**, 3541–3547; (*d*) M.-O. M. Piepenbrock, N. Clarke and J. W. Steed, *Langmuir*, 2009, **25**, 8451–8456.

14 (*a*) S. Ganta and D. K. Chand, *Dalton Trans.*, 2015, **44**, 15181–15188; (*b*) L. Yang, L. Luo, S. Zhang, X. Su, J. Lan, C.-T. Chen and J. You, *Chem. Commun.*, 2010, **46**, 3938–3940; (*c*) B. Xing, M.-F. Choi, Z. Zhou and B. Xu, *Langmuir*, 2002, **18**, 9654–9658; (*d*) X. Ma, S. Liu, Z. Zhang, Y. Niu and J. Wu, *Soft Matter*, 2017, **13**, 8882–8885.

15 (*a*) C. Po, Z. Ke, A. Y. Y. Tam, H. F. Chow and V. W. W. Yam, *Chem.–Eur. J.*, 2013, **19**, 15735–15744; (*b*) S. Ganta and D. K. Chand, *Inorg. Chem.*, 2018, **57**, 3634–3645; (*c*) P. Chen, Q. Li, S. Grindy and N. Holten-Andersen, *J. Am. Chem. Soc.*, 2015, **137**, 11590–11593.

16 (*a*) S. Dhibar, A. Dey, S. Majumdar, D. Ghosh, A. Mandal, P. P. Ray and B. Dey, *Dalton Trans.*, 2018, **47**, 17412–17420; (*b*) S. Dhibar, A. Dey, D. Ghosh, S. Majumdar, A. Dey, P. Mukherjee, A. Mandal, P. P. Ray and B. Dey, *ChemistrySelect*, 2019, **4**, 1535–1541; (*c*) S. Dhibar, A. Dey, S. Majumdar, A. Dey, P. P. Ray and B. Dey, *Ind. Eng. Chem. Res.*, 2020, **59**, 5466–5473; (*d*) S. Dhibar, A. Dey, S. Majumdar, P. P. Ray and B. Dey, *Int. J. Energy Res.*, 2021, **45**, 5486–5499; (*e*) S. Dhibar, S. K. Ojha, A. Mohan, S. P. C. Prabhakaran, S. Bhattacharjee, K. Karmakar, P. Karmakar, P. Predeep, A. K. Ojha and B. Saha, *New J. Chem.*, 2022, **46**, 17189–17200; (*f*) S. Dhibar, H. Dahiya, K. Karmakar, S. Kundu, S. Bhattacharjee, G. C. Nayak, P. Karmakar, G. D Sharma and B. Saha, *J. Mol. Liq.*, 2023, **370**, 121020; (*g*) S. Dhibar, A. Dey, A. Dalal, S. Bhattacharjee, R. Sahu, R. Sahoo, A. Mondal, S. M. Rahaman, S. Kundu and B. Saha, *J. Mol. Liq.*, 2023, **370**, 121021; (*h*) S. Dhibar, S. Babu, A. Mohan, G. K. Chandra, S. Bhattacharjee, K. Karmakar, P. Karmakar, S. M. Rahaman, P. Predeep and B. Saha, *J. Mol. Liq.*, 2023, **375**, 121348; (*i*) K. Karmakar, A. Dey, S. Dhibar, R. Sahu, S. Bhattacharjee, P. Karmakar, P. Chatterjee, A. Mondal and B. Saha, *RSC Adv.*, 2023, **13**, 2561–2569; (*j*) S. Dhibar, B. Pal, K. Karmakar, S. Kundu, S. Bhattacharjee, R. Sahoo, S. M. Rahaman, D. Dey, P. P. Ray and B. Saha, *ChemistrySelect*, 2023, **8**, e202204214.

17 (*a*) F. Gou, J. Cheng, X. Zhang, G. Shen, X. Zhou and H. Xiang, *Eur. J. Inorg. Chem.*, 2016, 4862–4866; (*b*) N. Kelly, K. Gloe, T. Doert, F. Hennersdorf, A. Heine, J. Marz, U. Schwarzenbolz, J. J. Weigand and K. J. Gloe, *Organomet. Chem.*, 2016, **821**, 182–191.

18 X.-Q. Wang, W. Wang, G.-Q. Yin, Y.-X. Wang, C.-W. Zhang, J.-M. Shi, Y. Yu and H.-B. Yang, *Chem. Commun.*, 2015, **51**, 16813–16816.

19 H. Bunzen, Nonappa, E. Kalenius, S. Hietala and E. Kolehmainen, *Chem.–Eur. J.*, 2013, **19**, 12978–12981.

20 B. Jiang, L.-J. Chen, G.-Q. Yin, Y.-X. Wang, W. Zheng, L. Xu and H.-B. Yang, *Chem. Commun.*, 2017, **53**, 172–175.

21 K. Mitsumoto, J. M. Cameron, R.-J. Wei, H. Nishikawa, T. Shiga, M. Nihei, G. N. Newton and H. Oshio, *Chem.–Eur. J.*, 2017, **23**, 1502–1506.

22 (*a*) Z. Yao, Z. Wang, Y. Yu, C. Zeng and K. Cao, *Polymer*, 2017, **119**, 98–106; (*b*) P. Rajamalli, P. Malakar, S. Atta and E. Prasad, *Chem. Commun.*, 2014, **50**, 11023–11025.

23 C. A. Offiler, C. D. Jones and J. W. Steed, *Chem. Commun.*, 2017, **53**, 2024–2027.

24 T. Feldner, M. Häring, S. Saha, J. Esquena, R. Banerjee and D. D. Díaz, *Chem. Mater.*, 2016, **28**, 3210–3217.

25 K. Mitsumoto, J. M. Cameron, R. -J. Wei, H. Nishikawa, T. Shiga, M. Nihei, G. N. Newton and H. Oshio, *Chem.–Eur. J.*, 2017, **23**, 1502–1506.

26 B. Xing, M.-F. Choi and B. Xu, *Chem.–Eur. J.*, 2002, **8**, 5028–5032.

27 J. Huang, L. He, J. Zhang, L. Chen and C.-Y. Su, *J. Mol. Catal. A: Chem.*, 2010, **317**, 97–103.

28 D. D. Díaz, D. Kuhbeck and R. J. Koopmans, *Chem. Soc. Rev.*, 2011, **40**, 427–448.

29 S. Sarkar, S. Dutta, S. Chakrabarti, P. Bairi and T. Pal, *ACS Appl. Mater. Interfaces*, 2014, **6**, 6308–6316.

30 Q. Lin, T.-T. Lu, X. Zhu, B. Sun, Q.-P. Yang, T.-B. Wei and Y.-M. Zhang, *Chem. Commun.*, 2015, **51**, 1635–1638.

31 S. Saha, E.-M. Schon, C. Cativiela, D. D. Diaz and R. Banerjee, *Chem.–Eur. J.*, 2013, **19**, 9562–9568.
32 H. B. Aiyappa, S. Saha, P. Wadge, R. Banerjee and S. Kurungot, *Chem. Sci.*, 2015, **6**, 603–607.
33 P. Grondin, O. Roubeau, M. Castro, H. Saadaoui, A. Colin and R. Clerac, *Langmuir*, 2010, **26**, 5184–5195.
34 V. R. Rajeev Kumar, V. Sajini, T. S. Sreeprasad, V. K. Praveen, A. Ajayaghosh and T. Pradeep, *Chem.–Asian J.*, 2009, **4**, 840–848.
35 D. Ljpez and J. M. Guenet, *Macromolecules*, 2001, **34**, 1076–1081.
36 R. D. Mukhopadhyay, G. Das and A. Ajayaghosh, *Nat. Commun.*, 2018, **9**, 1–9.
37 T. Ishi-I, R. Iguchi, E. Snip, M. Ikeda and S. Shinkai, *Langmuir*, 2001, **17**, 5825–5833.
38 P. Terech, V. Schaffhauser, P. Maldivi and J. M. Guenet, *Langmuir*, 1992, **8**, 2104–2106.
39 G. Behler, M. C. Feiters, R. J. M. Nolte and K. H. Dçtz, *Angew. Chem., Int. Ed.*, 2003, **42**, 2494–2497; *Angew. Chem.*, 2003, **115**, 2599–2602.
40 X. Wang, P. Duan and M. Liu, *Chem. Commun.*, 2012, **48**, 7501–7503.
41 K. Hanabusa, K. Hiratsuka, M. Kimura and M. H. Shirai, *Chem. Mater.*, 1999, **11**, 649–655.
42 (*a*) K. Araki and I. Yoshikawa, *Top. Curr. Chem.*, 2005, **256**, 133–165; (*b*) K. J. Skilling, A. Ndungu, B. Kellam, M. Ashford, T. D. Bradshaw and M. Marlow, *J. Mater. Chem. B*, 2014, **2**, 8412–8417; (*c*) B. Alies, M. A. Ouelhazi, A. N. Patwa, J. Verget, L. Navailles, V. Desvergnes and P. Barthelemy, *Org. Biomol. Chem.*, 2018, **16**, 4888–4894.
43 H. Svobodová, V. Noponen, E. Kolehmainen and E. Sievänen, *RSC Adv.*, 2012, **2**, 4985–5007.
44 C. Tomasini and N. Castellucci, *Chem. Soc. Rev.*, 2013, **42**, 156–172.
45 (*a*) R. Rajkamal, N. P. Pathak, D. Chatterjee, A. Paul and S. Yadav, *RSC Adv.*, 2016, **6**, 92225–92234; (*b*) A. Chalard, L. Vaysse, P. Joseph, L. Malaquin, S. Souleille, B. Lonetti, J.-C. Sol, I. Loubinoux and J. Fitremann, *ACS Appl. Mater. Interfaces*, 2018, **10**, 17004–17017.
46 M. Shibata, N. Teramoto and K. Kaneko, *J. Polym. Sci., Part B: Polym. Phys.*, 2010, **48**, 1281–1289.
47 J. K. Wolfe, R. M. Hann and C. S. Hudson, *J. Am. Chem. Soc.*, 1942, **64**, 1493–1497.
48 K. Hanabusa, K. Hiratsuka, M. Kimura and M. H. Shirai, *Chem. Mater.*, 1999, **11**, 649–655.
49 (*a*) B. Dahlke, S. Hellbardt, M. Paetow and W. H. Zech, *J. Am. Oil Chem. Soc.*, 1995, **72**, 349–353; (*b*) D. Swern, G. N. Billen, T. W. Findley and J. T. Scanlan, *J. Am. Chem. Soc.*, 1945, **67**, 1786–1789.
50 D. K. Smith, *Adv. Mater.*, 2006, **18**, 2773–2778.
51 P. Babu, N. M. Sangeetha and U. Maitra, *Macromol. Symp.*, 2006, **241**, 60–67.
52 Y. Wang, R. Tang, D. Wang, J. Wang, Y. Huang, Y. Ding, B. Lu, Y. Sun, P. J. Stang and Y. Yao, *Inorg. Chem.*, 2023, **62**, 1786–1790.
53 Y. Yao, R. Zhao, Y. Shi, Y. Cai, J. Chen, S. Sun, W. Zhang and R. Tang, *Chem. Commun.*, 2018, **54**, 8068–8071.
54 Y. Zhang, X. Yan, L. Shi, M. Cen, J. Wang, Y. Ding and Y. Yao, *Inorg. Chem.*, 2021, **60**, 7627–7631.
55 X. Miao, L. Piao and X. Kang, *Int. J. Polym. Mater. Polym. Biomater.*, 2023, **72**, 1112–1119.
56 D. Majumdar, J. E. Philip, S. Das, B. K. Kundu, R. V. Saini, G. Chandan, K. Bankura and D. Mishra, *J. Mol. Struct.*, 2021, **1225**, 129189.
57 S. Majumdar, G. Lepcha, K. T. Ahmed, I. Pal, S. R. Biswas and B. Dey, *J. Mol. Liq.*, 2022, **368**, 120619.
58 H. Ltaief, A. Mahroug, Y. B. Azaza, M. Nasri, M. P. Fernandes Graça and M. Belhouchet, *J. Mol. Struct.*, 2022, **1250**, 131829.
59 S. J. Sabounchei, M. Ahmadianpoor, A. Hashemi, F. Mohsenzadeh and R. W. Gable, *Inorg. Chim. Acta*, 2017, **458**, 77–83.
60 S. J. Sabounchei, F. A. Bagherjeri, C. Boskovic, R. W. Gable, R. Karamian and M. Asadbegy, *J. Mol. Struct.*, 2013, **1034**, 265–270.
61 (*a*) E. Eliuz, *Eurasian J. Forest Sci.*, 2020, **8**, 295–301; (*b*) T. Maji, S. Banerjee, A. Bose and T. K. Mandal, *Polym. Chem.*, 2017, **8**, 3164–3176; (*c*) S. A. Mohammad, S. Dolui, D. Kumar, S. R. Mane and S. Banerjee, *Biomacromolecules*, 2021, **22**(9), 3941–3949; (*d*) B. Xu, C. Feng, J. Hu, P. Shi, G. Gu, L. Wang and X. Huang, *ACS Appl. Mater. Interfaces*, 2016, **8**, 6685–6692.
62 P. Das, K. Tantubay, R. Ghosh, S. Dam and M. Baskey Sen, *Environ. Sci. Pollut. Res.*, 2021, **28**, 49125–49138.